

**EXPERIMENTAL STUDY OF OPTICALLY STIMULATED
LUMINESCENCE (OSL) DOSIMETRY TO THE DOSE
PERTURBATION OF 6MV PHOTON BEAM IN THE
PRESENCE OF METAL OBJECTS**

KONG WEI ZHEN

**SCHOOL OF HEALTH SCIENCES
UNIVERSITI SAINS MALAYSIA**

2024

**EXPERIMENTAL STUDY OF OPTICALLY STIMULATED
LUMINESCENCE (OSL) DOSIMETRY TO THE DOSE
PERTURBATION OF 6MV PHOTON BEAM IN THE
PRESENCE OF METAL OBJECTS**

by

KONG WEI ZHEN

**Dissertation submitted in partial fulfilment of the requirements for the degree of
Bachelor of Health Science (Honours) (Medical Radiation)**

July 2024

CERTIFICATION

I, Kong Wei Zhen, certify the dissertation entitled ‘EXPERIMENTAL STUDY OF OPTICALLY STIMULATED LUMINESCENCE (OSL) DOSIMETRY TO THE DOSE PERTURBATION OF 6MV PHOTON BEAM IN THE PRESENCE OF METAL OBJECTS’.

The research and writing of this dissertation have been performed under the supervision with the highest academic integrity. All sources used are appropriately cited and referenced. I hereby submit this dissertation for examination as part of the requirement for Bachelor of Health Science (Honours) (Medical Radiation) at UNIVERSITI SAINS MALAYSIA.

Main Supervisor,

Dr. Mohd Fahmi Bin Mohd Yusof

Lecturer

School of Health Sciences

Universiti Sains Malaysia

16150 Kubang Kerian

Kelantan, Malaysia

Date: 23rd July 2024

Co-Supervisor,

Cik. Arifah Nazirah Abdullah

Science Officer

School of Health Sciences

Hospital Universiti Sains Malaysia

16150 Kubang Kerian

Kelantan, Malaysia

Date: 23rd July 2024

DECLARATION

I declare that the work presented here is completely my own, excluding where due acknowledgment is made. The research and writing of this dissertation have been performed with the highest academic integrity. It has not been submitted for any other institutions. I grant Universiti Sains Malaysia the right to use this dissertation for any educational purposes.

KONG WEI ZHEN

Date: 23rd July 2024

ACKNOWLEDGEMENT

I would like to express my honest gratitude to all those who have contributed to the completion of this work. First and foremost, I would like to thank my main supervisor, Dr. Mohd Fahmi Bin Mohd Yusof for his invaluable guidance and advises throughout the this research project. Next, I am extremely grateful to my co-supervisor, Cik. Arifah Nazirah Abdullah for her forbearance, patience and assistances in completing this research work. Besides, special thanks to En. Ahmad Bazlie bin Abdul Kadir and Pn. Norriza Binti Mohd Isa for their expertise and guidance in the dosimetry study of optically stimulated luminescence dosimeters (OSLDs). They are the research officers of Malaysia Nuclear Agency under Secondary Standard Dosimetry Laboratories (SSDL). Furthermore, I sincerely appreciate the contributions from Pusat Pengajian Sains Kesihatan (PPSK) in providing materials and equipment to this research study. Finally, I am thankful to all those who have supported me in countless ways during my academic journey.

TABLES OF CONTENTS

CERTIFICATION	ii
DECLARATION	iii
ACKNOWLEDGEMENT	iv
TABLES OF CONTENTS	v
LIST OF TABLES	vii
LIST OF FIGURES	viii
LIST OF SYMBOLS	x
LIST OF ABBREVIATIONS	xi
LIST OF APPENDICES	xii
ABSTRAK	xiii
ABSTRACT	xv
CHAPTER 1	1
1.1 Background Study.....	1
1.2 Problem Statement.....	3
1.3 Significance of Study.....	3
1.4 Objective.....	4
1.4.1 General Objective:	4
1.4.2 Specific Objectives:	4
1.5 Hypothesis.....	5
1.5.1 Null Hypothesis	5
1.5.2 Alternative Hypothesis.....	5
1.6 Conceptual Framework.....	5
CHAPTER 2	6
2.1 Working Principles of Optically Stimulated Luminescence Dosimeter (OSLD).....	6
2.2 Dosimetric Study of Optically Stimulated Luminescence Dosimeters (OSLDs).....	7
2.3 Dosimetry Study of Radiotherapy Involving Metallic Implants.....	8
CHAPTER 3	10
3.1 Optically Stimulated Luminescence (OSL) Dosimetry System.....	10
3.1.1 Microstar Reader and Nanodot Dosimeter Calibrations	11
3.1.2 Intrinsic Checks and Initial Reading Measurements.....	13
3.2 Markus Plane-Parallel Ionization Chamber and Electrometer.....	14
3.3 Water-equivalent RW3 Slab Phantom.....	15
3.4 Metal Plates and Superflab Bolus	16
3.5 Dose Measurement Without Metal Plates.....	17

3.6 Dose Measurement in the Presence of Metal Plates	18
3.7 Study Flowchart.....	23
CHAPTER 4.....	25
4.1 Comparison of Percentage Depth Dose (PDD) Between OSLDs and Ionization Chamber Measurements	25
4.1.1 Comparison of Percentage Depth Dose (PDD) Between Ionization Chamber and OSL Dosimetry Without Metal Plates	25
4.1.2 Comparison of Percentage Depth Dose (PDD) Between Ionization Chamber and OSL Dosimetry in the Presence of 0.5cm Aluminium Plate	26
4.1.3 Comparison of Percentage Depth Dose (PDD) Between Ionization Chamber and OSL Dosimetry in the Presence of 1.0cm Aluminium Plate	28
4.1.4 Comparison of Percentage Depth Dose (PDD) Between Ionization Chamber and OSL Dosimetry in the Presence of 1.0 cm Lead Plate	29
4.1.5 Discussion	31
4.2 Dose Perturbation in the Presence of Metal Plates	32
4.2.1 Dose Perturbation in the Presence of 0.5cm Aluminium Plate	32
4.2.2 Dose Perturbation in the Presence of 1.0 cm Aluminium Plate	34
4.2.3 Dose Perturbation in the Presence of 1.0 cm Lead Plate	36
4.2.4 Discussion	37
CHAPTER 5.....	43
CHAPTER 6.....	44
REFERENCES.....	45
APPENDICES.....	51
APPENDIX A	51
APPENDIX B.....	53
APPENDIX C.....	57
APPENDIX D.....	62

LIST OF TABLES

Table 3.1: Table 3.1: Physical characteristics of metal plates.....	16
Table 4.1: PDD measured by IC and OSLDs without metal plates.....	25
Table 4.2: Results of Mann-Whitney test for PDD measured by IC and OSL without metal plate.....	25
Table 4.3: PDD measured by IC and OSLDs in the presence of 0.5 cm aluminium plate....	26
Table 4.4: Results of Mann-Whitney test for PDD measured by IC and OSLDs in the presence of 0.5 cm aluminium plate.....	26
Table 4.5: PDD measured by IC and OSLDs in the presence of 1.0 cm aluminium plate...	28
Table 4.6: Results of Mann-Whitney test for PDD measured by IC and OSLDs in the presence of 1.0 cm aluminium plate.....	28
Table 4.7: PDD measured by IC and OSLDs in the presence of 1.0 cm lead plate.....	29
Table 4.8: Result of Mann-Whitney test for PDD measured by IC and OSLDs in the presence of 1.0 cm lead plate.....	29
Table 4.9: PDD of OSL measurements with and without the presence of 0.5 cm aluminium plate.....	33
Table 4.10: BSDF and FDPF of OSL measured doses in the presence of 0.5 cm aluminium plate.....	34
Table 4.11: PDD of OSL measurements with and without the presence of 1.0 cm aluminium plate.....	35
Table 4.12: BSDF and FDPF of OSL measured doses in the presence of 1.0 cm aluminium plate.....	35
Table 4.13: PDD of OSL measurements with and without the presence of 1.0 cm lead plate.....	36
Table 4.14: BSDF and FDPF of OSL measured doses in the presence of 1.0 cm lead plate.	37
Table C.1: Raw data of OSLDs readout.....	58
Table C.2: Raw data of IC charges without metal plates.....	61
Table C.3: Raw data of IC charges in the presence of 0.5 cm aluminium plate.....	61
Table C.4: Raw data of IC charges in the presence of 1.0 cm aluminium plate.....	62
Table C.5: Raw data of IC charges in the presence of 1.0 cm lead plate.....	62

LIST OF FIGURES

Figure 1.1: Conceptual Framework.....	5
Figure 3.1: Nanodot OSL-based dosimeters.....	11
Figure 3.2: Microstar reader with an external PC.....	11
Figure 3.3: Irradiation setup for nanodot dosimeters.....	13
Figure 3.4: High and low dose calibration factor.....	13
Figure 3.5: Annealing of nanodot dosimeters.....	14
Figure 3.6: Markus plane-parallel ionization chamber.....	15
Figure 3.7: RW 3 solid water phantom.....	16
Figure 3.8: Aluminium and lead plates with different thicknesses.....	16
Figure 3.9: Alignment of the IC adapter plate to the lasers.....	18
Figure 3.10: Placement of nanodot dosimeters at the cross-hair of the light beam.....	30
Figure 3.11: Dose measurements in the presence of 0.5 cm aluminium plate.....	19
Figure 3.12: Dose measurements in the presence of 1.0 cm aluminium plate.....	20
Figure 3.13: Dose measurements in the presence of 1.0 cm lead plate.....	20
Figure 3.14: Centralization of 0.5 cm aluminium plate to the cross-hair of the light field.....	22
Figure 3.15: IC measurements in the presence of metal plates.....	18
Figure 3.16: OSL measurements in the presence of metal plates.....	18
Figure 4.1: PDD of IC and OSL measurements without metal plates.....	25
Figure 4.2: PDD of IC and OSL measurements in the presence of 0.5 cm aluminium plate...26	26
Figure 4.3: PDD of IC and OSL measurements in the presence of 1.0 cm aluminium plate...28	28
Figure 4.4: PDD of IC and OSL measurements in the presence of 1.0 cm lead plate.....29	29
Figure 4.5: PDD of OSL measurements with and without the presence of 0.5 cm aluminium plate.....	32
Figure 4.6: PDD of OSL measurements with and without the presence of 1.0 cm aluminium plate.....	34
Figure 4.7: PDD of OSL measurements with and without the presence of 1.0 cm lead plate.....	36
Figure A.1: Mann-Whitney test for PDD of IC and OSL measurements without metal plates.....	52
Figure A.2: Mann-Whitney test for PDD of IC and OSL measurements in the presence of 0.5 cm aluminium plate.....	52

Figure A.7: Mann-Whitney test for PDD of IC and OSL measurements in the presence of 1.0 cm aluminium plate.....	53
Figure A.8: Mann-Whitney test for PDD of IC and OSL measurements in the presence of 1.0 cm lead plate.....	53
Figure B.1: Asymmetrical distribution of PDD measured by IC and OSLDs without metal plates.....	54
Figure B.2: Asymmetrical distribution of PDD measured by IC and OSLDs in the presence of 0.5 cm aluminium plate.....	55
Figure B.3: Asymmetrical distribution of PDD measured by IC and OSLDs in the presence of 1.0 cm aluminium plate.....	56
Figure B.4: Asymmetrical distribution of PDD measured by IC and OSLDs in the presence of 1.0 cm lead plate.....	57
Figure D.1: Certificate of calibration for Markus plane-parallel ionization chamber.....	62
Figure D.2: Certificate of irradiation of OSL dosimeters.....	63
Figure D.3: Certificate of irradiation of OSL dosimeters.....	64

LIST OF SYMBOLS

PDD_h	Percentage Depth Dose without metal plates
$PDD_{0.5Al}$	Percentage Depth Dose with 0.5 cm aluminium plates
$PDD_{1.0Al}$	Percentage Depth Dose with 1.0 cm aluminium plates
$PDD_{1.0Pb}$	Percentage Depth Dose with 1.0 cm lead plates
PDD_{OSL}	Percentage Depth Dose measured by nanodot dosimeters
PDD_{IC}	Percentage Depth Dose measured by ionization chamber
Z	Atomic number
D_i	Dose in the presence of metal plates
D_h	Dose without the presence of metal plates
D_{OSL}	Dose measured by OSLDs
D_{IC}	Dose measured by IC

LIST OF ABBREVIATIONS

OSL	Optically Stimulated Luminescence
OSLDs	Optically Stimulated Luminescence Dosimeters
IC	Ionization Chamber
CT	Computed Tomography
PDD	Percentage Depth Dose
PMT	Photomultiplier Tube
ANM	Malaysia Nuclear Agency
PSDL	Primary Standards Dosimetry Laboratory
SSDL	Secondary Standard Dosimetry Laboratory
SPSS	Statistical Package for Social Sciences
TPS	Treatment Planning System
MC	Monte-Carlo
CV	Coefficient of Variations
CPE	Charged Particle Equilibrium
DPF	Dose Perturbation Factor
BSDF	Backscattered Dose Perturbation Factor
FDPF	Forward Dose Perturbation Factor
MLC	Multileaves

LIST OF APPENDICES

APPENDIX A	Results of Mann-Whitney tests for comparisons of PDD between OSLDs and IC dosimetry
APPENDIX B	Result of normality tests
APPENDIX C	Raw data of OSLDs and IC measurements
APPENDIX D	Certificate of irradiation of IC

KAJIAN EKSPERIMEN DOSIMETRI LUMINENS STIMULASI OPTIK (OSL) TERHADAP PERTURBASI DOS FOTO 6MV DENGAN KEHADIRAN OBJEK LOGAM

ABSTRAK

Prevalens implan logam telah membawa cabaran yang besar semasa radioterapi disebabkan oleh interaksi foton dengan logam. Implan logam boleh mengubah distribusi dos yang diinginkan dalam badan pesakit, mengakibatkan gangguan dos dan seterusnya rawatan yang tidak berkesan. Dosimeter nanodot komersial yang berdasarkan teknik luminens stimulasi optik (OSL) telah muncul sebagai dosimetri alternatif dalam bidang radioterapi disebabkan sensitiviti tinggi, kebolehgunaan semula dan saiz kecilnya. Kajian ini bertujuan untuk menyiasat gangguan dos dari sinaran foton akibat objek logam dengan menggunakan dosimeter nanodot. **Kaedah:** Kajian eksperimental ini telah dijalankan untuk membandingkan dos dan peratusan dos kedalaman (PDD) dari ukuran kebuk pengion Markus dan dosimeter nanodot dalam phantom air pepejal ketebalan 20 cm dengan dan tanpa plat plumbum 1.0 cm, plat aluminium 0.5 cm dan 1.0 cm. Gangguan dos disebabkan oleh plat logam juga disiasat. **Keputusan:** Nilai-p dari ujian 'Mann-Whitney' untuk perbandingan dos dan PDD antara ukuran dosimeter nanodot dan kebuk pengion Markus semuanya lebih besar daripada 0.05. Ketidakpastian statistik dari sistem dosimetri nanodot adalah sehingga 13.75%, iaitu lebih besar daripada 3% yang diterbitkan daripada laporan IAEA TRS no 398. Faktor gangguan dos terserak belakang (BSDF) adalah lebih tinggi daripada 1.0 dari kedalaman 4.0 cm sehingga permukaan 0.5 cm plat aluminium (1.01 – 1.03) dan 1.0 cm plat aluminium (1.03 - 1.03) manakala ia lebih tinggi daripada 1.0 dari kedalaman 2.5 cm sehingga permukaan 1.0 cm plat plumbum (1.02 - 1.16). Julat faktor gangguan dos hadapan (FDPF) untuk pengukuran dos di belakang 0.5 cm dan 1.0 cm plat aluminium ialah 0.96 – 0.98 dan 0.93-0.96 masing-masing..

Julat FDPF di belakang 1.0 cm plat plumbum ialah 0.57-0.67. **Kesimpulan:** Tiada perbezaan yang ketara antara dosimetri OSL dan IC dalam pengukuran dos dengan dan tanpa plat logam. Ketidakpastian yang tinggi dalam dosimetri OSL adalah disebabkan oleh ketepatan sistem dosimetri OSL yang tidak memuaskan. Dosimetri OSL berupaya mengukur perubahan dos, BSDF dan FDPF didapati lebih signifikan dengan peningkatan nombor atom logam.

**EXPERIMENTAL STUDY OF OPTICALLY STIMULATED
LUMINESCENCE (OSL) DOSIMETRY TO THE DOSE
PERTURBATION OF 6MV PHOTON BEAM IN THE PRESENCE OF
METAL OBJECTS**

ABSTRACT

The prevalence of metallic implants have brought significant challenges during radiation therapy due to the photon interaction with metal. Metallic implants can alter the desired dose distribution within patient bodies, resulting in dose perturbation and consequently ineffective treatment delivery. Commercial nanodot dosimeters based on Optically Stimulated Luminescence (OSL) techniques has emerged as an alternative dosimetry method in radiotherapy due to their high sensitivity, reproducibility and small sizes. This study aims to investigate the dose perturbation of high photon beam in the presence of metal objects using nanodot OSL-based dosimeters. **Method:** An experimental study was conducted to compare the doses and Percentage Depth Dose (PDD) measured by Markus ionization chamber and nanodot dosimeters in a 20 cm thickness solid water phantom with and without the presence of 1.0 cm lead plate, 0.5 cm and 1.0 cm aluminium plates from which the dose perturbation due to metal plates was investigated as well. **Results:** The p-values from the Mann-Whitney test for comparisons of measured doses and PDD between OSL and IC measurements are all greater than 0.05. However, statistical uncertainties of nanodot dosimetry system are up to 13.75%, which is greater than the desired 3% published from IAEA TRS report no 398. When measuring dose with a 0.5 cm aluminium plate, BSDF values exceed 1.0 at a depth of 4 cm (BSDF = 1.01), using 1 cm aluminium plate increase the BSDF to 1.03 at 4 cm depth. Switching to a 1 cm lead plate results in BSDF exceeding 1.0 at a depth of 2.5 cm (BSDF = 1.02). The ranges of FDPF

for dose measurements with 0.5 cm and 1 cm aluminium plate are 0.96 – 0.98 and 0.93 – 0.96 respectively. The FDPF range behind the lead plate is 0.57-0.67. **Conclusion:** There is no a significant difference between OSL and IC dosimetry in measurements with and without metal plate. The higher uncertainties of nanodot dosimetry is due to the unsatisfied precision of the nanodot dosimetry system This research demonstrated that OSL dosimetry is effective in measuring dose perturbations, with BSDF and FDPF becoming more significant as the atomic number of the metal increases.

CHAPTER 1

INTRODUCTION

1.1 Background Study

Metallic implants have become a solution for many medical conditions and injuries. They can be classified into orthopedic implants which serve to replace or support the damaged bony structures such as hip, knee, elbow and shoulder. Dental implants literally replace the broken teeth and act as an anchor for dental prosthetics, such as amalgam tooth fillings, crowns and bridges. Pacemaker as an implantable devices on patient`s heart to maintain a normal heart beat and rhythm is also made of metallic materials. Therefore, metallic implants that become a part of patient body, playing an important role in maintaining the daily body functioning and even keep patients` lives. Problem arises when patients with metallic implants come for radiotherapy. The metal objects lead to beam hardening, noise and scattered radiation in the acquired CT images during simulation, causing changes in the attenuation characteristics of the material being imaged, thus delivering an overestimated attenuation coefficient (very high density) of the metal objects, resulting in a substantial increase of high Hounsfield unit (HU). These finally result in metal artifacts on the CT images, causing difficulties in delineating the organs and tumor volume and decreased accuracy in dose calculation (Barreto et al., 2020). Besides, the presence of metallic implants will create a metal heterogeneity that drastically vary the dose distribution. This is because metallic implants made of high atomic number will attenuate the high energy photon beams, leaving an underdose and overdose area near the metallic implants. This situation is called dose perturbation (Zhao et al., 2020). The high atomic number of metal objects will increase backscattering of radiation, leading to increase in dose near the entry of metal objects, the probability of photoelectric absorption and pair production also increase with high atomic number, which absorbing the radiation severely, leaving an underdose region behind the implants (Fèvre et al., 2022). Therefore, treatment goal will be affected due to the

non-uniform dose distribution onto the planning target volume (PTV) no matter the PTV is in front or behind the implants. Clinically, electron beam is more susceptible to dose perturbation by metallic implants due to their relatively low mass that make them prone to interactions with material they pass through (Sarigul, 2022). Dosimetry of the delivered dose in the presence of metallic implants is therefore important to know the dose perturbation and actual dose delivered to the planning target volume (PTV). Ionisation chambers measurement in a phantom is a standard method used by many author to evaluate the dose perturbation of high energy photon beam in the presence of metal objects (Heng et al., 2021; Khaleghi et al., 2021).

Optically Stimulated Luminescence (OSL) technique is well-known for occupational dose monitoring since 1998. Nanodot OSL-based dosimeter is a commercial OSLDs composed of plastic disks infused with aluminium oxide doped with carbon ($\text{Al}_2\text{O}_3:\text{C}$) crystals and encased in a light tight plastic holder. Its working principle is based on the electron traps in the crystalline dielectric materials during the exposure, the stored energy of the trap can be released by light stimulation, emitting as luminescence and measured by photomultiplier tube (PMT) in a reader to determine the radiation dose (Lopes et al., 2022). Nanodot dosimeters currently gain popularity in term of patient dosimetry in radiotherapy due to its fast measurement, high sensitivity, reproducibility, compact design, readability, and the ability of long-term dose storage (Eddam & Krishnan, 2024). They are used as secondary patient dose verification for in-vivo dosimetry and quality assurance. Their compact design make them available to measure the point dose distribution anywhere of patient body such as eye dose measurement (Gasparian et al., 2022; Chun et al., 2022; Solomon et al., 2020). Nanodot dosimetry does not require a holder, heating parameters, nitrogen gas and no wire to be connected to the monitor, these easy setup make them well suited for both clinical and research applications especially the phantom studies. Besides, the wide energy range (5 keV-20 MeV) makes them a comparable dosimetry method in diagnostic radiology for patient dosimetry. There are some technological

advancements in OSL dosimetry for a more reliable and fast readout. For examples, a build-up cap is added to the active element of OSLD for accurate measurement of surface doses and a introduction of a newly-developed $\text{MgB}_4\text{O}_7:\text{Ce}^{3+},\text{Na}^+$ phosphor materials with higher sensitivity and better stability (Riegel et al., 2017; Ozdemir et al., 2021).

1.2 Problem Statement

The presence of metallic implants lead to a metal heterogeneity and bring significant challenges in ensuring an accurate dose delivery due to the dose perturbation that cause potentially underdosing and overdosing of surrounding tissues near the metal object, causing non-uniform dose distribution and thus compromising patient outcome. There are many literature studying the backscattering effects of electron and photon beam from the high density metal objects. However, the impacts on dose perturbation of high energy photon beam before and behind the metal objects remains insufficiently understood. Nanodot OSL-based dosimeters are known for its sensitivity, precision, and reusability in medical dosimetry, however, applications of OSL dosimetry in the presence of metal objects has not been extensively explored. The existence of metal objects will cause a drastic change of energy spectrum of radiation which lead to a complex dose gradient around the metal, thus requiring the dosimeters to be sensitive enough the capture the variation precisely (Fèvre et al., 2020). Furthermore, the TPS algorithms such as pencil beam (PB) or the collapsed cone (CC) might not perfectly model the dose perturbation near the heterogeneous regions especially metallic implants compared to local measurement by dosimeters (Chopra et al, 2018). It is invasive and impractical as well to insert or implant the nanodot dosimeters inside the patient bodies to measure the dose perturbation around the metallic implants.

1.3 Significance of Study

Since TPS is not a desired method for local dosimetry of dose perturbation plus nanodot dosimeters cannot be inserted into patients, there is a need for an experimental study to quantify

the dose perturbation of high energy photon beam in the presence of metal objects by using a solid water phantom. This study will also investigate the contribution of dose perturbation from backscattering of the radiation in front of metal and forward scattering of radiation behind the metal. This will improve the knowledge gap due to insufficient researches about the dose perturbation of high energy photon beam in the presence of metallic implants, providing new insights that can inform clinical practice. Furthermore, the accuracy and precision of nanodot OSL-based dosimeters in capturing complex dose gradients due to the dose perturbation by metal objects will be studied as well and then come out with improved OSL dosimetric technique in measuring dose perturbation by metal objects.

1.4 Objective

1.4.1 General Objective:

To investigate Optically Stimulated Luminescence (OSL) dosimetry to the dose perturbation of high energy photon beam in the presence of metallic objects.

1.4.2 Specific Objectives:

- i. To compare the Percentage Depth Dose (PDD) with and without the presence of metal plates between Optically Stimulated Luminescence Dosimeters (OSLDs) and Markus ionization chamber
- ii. To determine the backscattered dose perturbation factor (BSDF) near the entrance of high-low density interfaces using Optically Stimulated Luminescence Dosimeter (OSLD) measurements
- iii. To determine the forward dose perturbation factor (FDPF) near the exit of high-low density interfaces using Optically Stimulated Luminescence Dosimeter (OSLD) measurements

1.5 Hypothesis

1.5.1 Null Hypothesis

There is no significant difference of Percentage Depth Dose (PDD) between Optically Stimulated Luminescence Dosimeters (OSLDs) and Markus ionization chamber measurements.

1.5.2 Alternative Hypothesis

There is a significant difference of Percentage Depth Dose (PDD) between Optically Stimulated Luminescence Dosimeters (OSLDs) and Markus ionization chamber measurements.

1.6 Conceptual Framework

The independent variables of this study are nanodot OSL-based dosimeters and Markus ionization chamber. They are used to measure the dependent variables, which are doses, PDD, BSDF and FDPF. Do note that BSDF and FDPF are determined from OSLDs measurement only due to its availability in measurement closet to the high-low density interface. 0.5 cm aluminium plate, 1.0 cm aluminium plate and 1.0 cm lead plate are the moderating variables that influence the doses and PDD measured by nanodot dosimeters and IC. Figure 1.1 illustrates the conceptual framework used to determine the significant differences between the doses and PDD measured by nanodot dosimeters and IC.

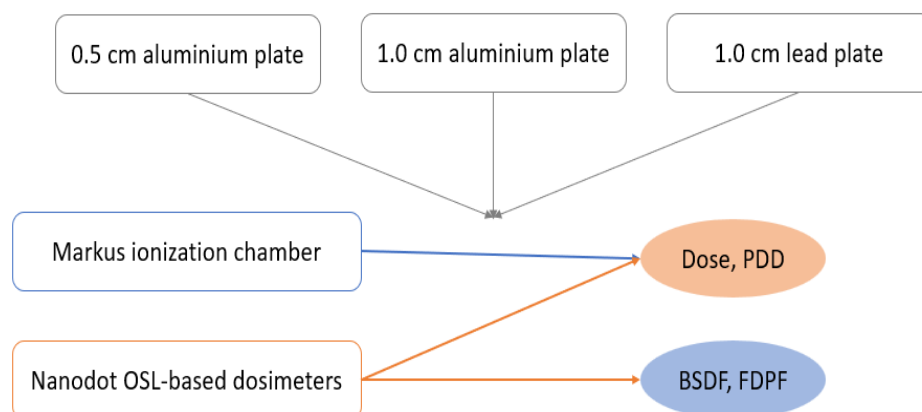


Figure 1.1: Conceptual Framework

CHAPTER 2

LITERATURE REVIEW

2.1 Working Principles of Optically Stimulated Luminescence Dosimeter (OSLD)

Nanodot OSL-based dosimeter is a flat plastic cassette (10mm x 10mm) that contains a 7mm diameter and 0.3mm-thick plastic disk coated with a pure crystalline dielectric material. It is based on Optically Stimulated Luminescence (OSL) technology. The energy level in the crystalline structure consists of valence and conduction band separated by a band gap, called forbidden gap. Energy states are forbidden in this gap, no electrons. Hence, the crystal usually contains contaminants which is intentionally introduced to form crystal-lattice imperfections (defects) that acts as electron traps or luminescence centers in the forbidden gap (Jursinic, 2007). The most common crystals used in OSL dosimeter is aluminium oxide doped with carbon ($\text{Al}_2\text{O}_3:\text{C}$). Carbon is the impurities added to the crystal lattice. When exposing the crystal to ionising radiation, the electrons in the valence band are excited to the conduction band, leaving a hole in the valence band. The electrons in the conduction band and the holes in the valence band are free to move in the crystal lattice. Free electrons can be trapped, producing filled electron traps. Three electron traps are found, which are shallow, dosimetry and deep traps. These traps literally refer to different 'trap levels' of the electrons (Kry et al., 2019). Extra electrons in the hole traps fill the holes in the valence band and the holes from the valence band fill the hole traps, creating filled hole traps, which are F center (recombination/luminescence center) and the electrons originally at the hole traps will be trapped at the electron traps, which have higher energy level and producing filled electron traps. The greater the intensity of the radiation, the more the filled electron traps. The electrons can be released by optical stimulation with visible light such as green light in a reader during the readout of OSL dosimeter. The released electrons can move through the conduction band to the hole traps. Now the hole traps achieve excited state, having charges (+1), turning from F center to F^+ center. At the F^+ center,

the electron recombine with the hole and the recombination energy is transferred to the F^+ center where light (luminescence) is emitted (Chun et al., 2022). Other than recombination, luminescence can be produced by de-excitation of the trapped electrons. This happens when the valence band electron absorbed the light energy, moving to the filled hole trap and leaving a vacancy in the valence band. The trapped electrons fill the vacancies and luminescence is produced. The intensity of luminescence depends on the number of filled electron traps which in turn depend on the intensity of radiation absorbed. The number of luminescence is counted by photomultiplier tube (PMT) and expressed as ‘counts’. In fact, shallow electron traps are unstable at ambient temperature, the captured electrons can be released within a few minutes at room temperature even without optical stimulation, resulting in phosphorescence that cause initial increase of OSL signals. Hence, there must be a delay between dosimeter irradiation and readout to reduce the phosphorescence signal (Kry et al., 2019). Dosimetric electron traps can hold the electrons at room temperature for more than 100 days and release the electrons when being stimulated by visible light with 390–780 nm wavelength. Luminescence from this traps are the main OSL signal for dosimetry or dose determination. For deep electron traps, the electrons can be released only at very high temperatures (700–1000 °C) or with ultraviolet irradiation. This is referred to as bleaching (zeroing) that aims to empty the electron traps. Hence, OSL dosimeter can be reseted and reused for subsequent dose measurement (Park et al., 2017).

2.2 Dosimetric Study of Optically Stimulated Luminescence Dosimeters (OSLDs)

Optically Stimulated Luminescent Dosimeters (OSLDs) have become more and more important in radiotherapy due to their high sensitivity, accuracy, and small sizes. Yusof et al. (2017) verified OSLD doses in low and high energy x-ray by comparing to ionization chamber and thermoluminescent dosimeters (TLD100). They reported that OSLD doses were less in agreement to ionization chamber compared to that in TLD100 in low energy x-ray and was in

good agreement to that in ionization chamber at high energy x-ray. The dose measured using OSLD were found to be more consistent at high energy x-ray as shown by the smaller standard deviation of the readings. Besides, Yusof et al. (2020) also compared the PDD measurements between OSLDs and IC in 6 and 10 MV photons and 9 and 12 MeV electrons at 3×3 cm field sizes. They reported that PDD_{OSL} in lower photon and electron energies were in good agreement within 4% PDD_{IC} . PDD_{OSL} in 10 MV photons showed gradual increase of deviation up to 10% beyond the depth of maximum dose (d_{max}). The surface doses in OSL dosimeters were significantly higher compared to IC measurement. Other than ionization chamber, Wong et al. (2019) compared PDD_{OSL} with Monte-Carlo (MC) simulation and found that PDD_{OSL} is slightly lower than PDD of MC simulation, the total uncertainty in a single dose measurement was 11% and could be reduced to 9.2% when energy dependence correction was applied. These researches had successfully justified OSL dosimetry as an alternative dosimetry method in radiotherapy but did not study its response to dose perturbation caused by the presence of metal objects.

2.3 Dosimetry Study of Radiotherapy Involving Metallic Implants

In the literature, researchers verified radiotherapy dose calculation at the high-low density interfaces via TPS algorithms, MC simulations and other dosimetric techniques including dosimeters. Biggs and Russell (1988) used an ionisation chamber (IC) to measure the dose through the head of hip prosthesis and reported an average decrease of approximately 2% of prescribed dose behind the prostheses for 25 MV X rays and average increases of approximately 2% dose close to the upstream surface of the prosthesis for 10 MV X rays. This research studied the dose perturbation up to 25 MV photon beam but limited to IC dosimetry only. Similar findings on dose perturbation near the high-low density interface were also reported by other authors using measurements with either IC, EBT3 film, or treatment planning system (TPS) with different algorithms such as pencil beam, superposition and Analytical

Anisotropic Algorithm (AAA) (Reft et al, 2003; Alhakeem et al, 2015). Backscattered Dose Perturbation Factor (BSDF) and Forward Dose Perturbation Factor (FDPF) were studied by Reft et al. (2003) through a slab inhomogeneity (bone, steel and lead) using 6 photon beams in a water-equivalent phantom. They found that FDPF varied from 0.94 to 0.84 for bone and lead in 6 MV photon beam and BSDF varied from 1.05 to 1.41 for bone and lead respectively. Besides, these correction factors were independent of the depth of the high atomic number material but FDPF was dependent on beam energy. This results agreed with the findings of Rajamanickam et al. (2018) and Mohammadi et al. (2017), both of them also studied the dosimetric properties of megavoltage (MV) beams on high Z implant materials.

There was indeed a very limited literature studying OSLD dosimetry in the presence of metallic implants. Ispir et al. (2021) evaluated OSL dose measurement in the presence of metal implants by comparing nanodot PDD at different high-low interfaces with EBT3 film, ionisation chamber, Monte-carlo (MC) simulations and Acuros XB (AXB) algorithm. They reported mean relative differences of 2.5%, 5.6%, and 9.8% between OSLD and MC simulation at the entry interfaces between slab phantom and aluminium plate, titanium alloy, stainless steel grade respectively, the PDD dose of OSLDs were similar to MC calculation at the exit interface of high-low density. This research verified the OSL dosimetry with different measurement techniques but the study was limited to small field sizes and the photon energies were up to 10 MV only. Serichetaphongse and Kunapinun (2022) compared the back- and forward-scattered doses from nine contemporary dental materials made of different noble alloy groups, they applied nanodot-OSL dosimeters due to the ease of placement above and below for back- and forward-scattered dose measurement. However, there was no verification of OSL dosimetry with other dosimetry technique. Hence, there was a research gap due to the lack of existing literature on OSLD dosimetry or the verification of OSL dosimetry in the presence of metallic objects.

CHAPTER 3

MATERIAL & METHODS

This was an experimental study on OSL dosimetry to dose perturbation of high energy photon beam in the presence of metal objects. The venue of the research project was the Radiotherapy & Oncology Department of Hospital Universiti Sains Malaysia (HUSM). The study was carried out under the supervision of a medical physicist, Miss Arifah Nazirah Abdullah. The materials used in this study were nanodot OSL-based dosimeters, MicroStar reader, Markus ionisation chamber, solid water phantom, Varian RapidArc linear accelerator (LINAC), superflab bolus, aluminium and lead plates. A total of 57 commercial nanodot OSL-based dosimeters and a MicroStar reader were involved in the research. The dose range of nanodot dosimeters is from 50 μ Gy to 1500cGy while the energy range is from 5 keV to 20 MeV.

3.1 Optically Stimulated Luminescence (OSL) Dosimetry System

The OSL dosimetry system includes a InLight® Laundauer microStar reader incorporating with an external personal computer (PC), installed with a special software to read the measurement with optically stimulated luminescence (OSL) technology and exporting to Microsoft Excel spreadsheet for analysis. The 2D barcode scanner is used to scan the nanodot dosimeter for readout process. The dot dosimeter (nanodot) consists of an OSL active crystal with 7 mm diameter and 0.3 mm thickness, encased in a lightproof plastic housing with 10 mm \times 10 mm \times 2 mm dimension and mass density of 1.03 g/cm³. The front and back of the OSLD disks are covered with plastic sheets of 0.36mm thickness. The housing will be automatically opened during the readout process in the reader and could be opened manually for annealing. The microstar reader is operated in two modes with different powers of light stimulation depending on the amount of stored dose in the dosimeter. The nanodot dosimeter will first be stimulated with a low power of light beam and then monitor the initial response. If the initial response is large enough (high doses), the reading process continues, otherwise a high power

beam is used to get a signal large enough to measure small doses (Mrčela et al, 2011). For OSLDs readout, first, the reading tab was opened on the PC, a 2D barcode scanner was used to scan the QR code of the nanodot dosimeters. The scanned dosimeters were placed in an adapter and then put into the loader of the reader. The rotary knob of the reader was turned from the home position (H/P) clockwise into the reading position (E1) to open the housing of OSL dosimeter for light exposure. Turning back to the home position closed the housing and allowed withdrawing the loader. OSL readings were displayed in the Import/Export tab and then exporting the data into an excel file.



Figure 3.1: Nanodot OSL-based dosimeter



Figure 3.2: Microstar reader with an external PC

3.1.1 Microstar Reader and Nanodot Dosimeter Calibrations

Calibration of radiation measuring instruments is placed under the Atomic Energy Licensing Act 1984 (Act 304), Radiation Protection (Basic Safety Standards) Regulations 1988 (amended 2010) to ensure the accuracy and reliability of the dose measurement. In this case, 15 nanodot

dosimeters were calibrated by pre-irradiating to low doses (0, 6mGy, 30mGy) and high doses (500mGy, 1000mGy). The irradiation setup is shown in Figure 3.3 in which the OSL dosimeters were put on the surface of a solid water phantom. This setup was applied to the irradiation of a farmer-type ionization chamber as well. The measured dose by OSL dosimeter need to be calibrated to a reference dose measured by an ionization chamber (gold standard) that is calibrated traceably with Secondary Standards Dosimetry Laboratory (SSDL). SSDL was established by The International Atomic Energy Agency (IAEA) and World Health Organization (WHO), SSDL in Malaysia is located in Malaysia Nuclear Agency (ANM). For reader calibration, traceability of radiation measurements to the SI units were done through the network of SSDL to improve the accuracy in radiation dosimetry (IAEA, 2007). MicroStar reader was calibrated with those 15 preirradiated nanodot dosimeters to determine the calibration factors for converting the raw PMT count to dose (mSv). During the reader calibration, calibration tab was opened on the PC and create a low dose calibration type and labelled as ‘Therapy’. This low dose calibration factor corresponded to the OSL dosimeters exposed to low doses (0, 6mGy, 30mGy). Then read the preirradiated OSL dosimeters, the readout process was the same as section 3.1 but this was done in the calibration tab. The steps were repeated for the dosimeters exposed to high doses (500mGy, 1000mGy) but a high dose calibration type was set. Then saving the high and low dose calibration factor (counts/mGy) in the laptop to be used for future readout.

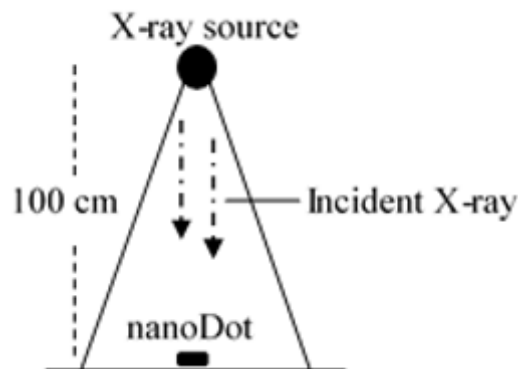


Figure 3.3: Irradiation setup for nanodot dosimeters



Figure 3.4: Low and high dose calibration factors

3.1.2 Intrinsic Checks and Initial Reading Measurements

Intrinsic measurements aims to access the performance and stability of the reader in terms of dark counts, photomultiplier tube (PMT) counts and photodiode (P-Diode) counts. Dark counts are those PMT counts detected in the absence of radiation and it is due to the light leakage within the reader. PMT counts are the signals counted when PMT is irradiated with the internal LED light, its stability for routine use is influenced by both PMT and LED. Photodiode counts reflect the LED light so it is useful in assessing the LED stability (Mrčela et al, 2011). Intrinsic measurement of the reader must be performed before the readout to ensure the dark counts were less than 10 average counts, coefficient of variation (CV) of photomultiplier tube (PMT) counts and photodiode (P-Diode) counts were ensured to be within $\pm 10\%$.

During the calibration of nanodot dosimeters, each of them was pre-irradiated to a known dose to establish a baseline signal, which served as initial readings for the subsequent measurements. The initial readings also involved the background signal due to the dosimeter exposures to the environmental radiation. For actual measurements in this study, the measured doses obtained was subtracted with the initial reading to get an accurate reading. Before the next measurement, nanodot dosimeters were annealed to remove the residual signals from previous exposure and reset the dosimeter back to the baseline state. Then initial readings were taken to be subtracted from the next measurements. The process of annealing and initial reading measurements must be done prior to the next measurements. Nanodot dosimeters were always

kept in a dark box because OSLDs are highly sensitive to light, the light stimulation will release the trapped electrons which lead to luminescence that alter the stored dose information. It also helped prevent the background exposures.

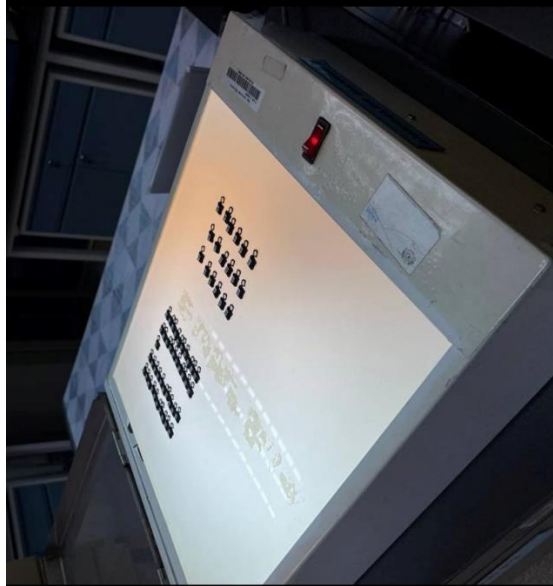


Figure 3.5: Annealing of nanodot dosimeters

3.2 Markus Plane-Parallel Ionization Chamber and Electrometer

Ionization chamber measurement was used in this experimental study as a reference measurement for the verification of OSL dosimetry. This is because ionization chamber can provide a highly accurate, precise and real-time dose measurement (Kesen et al, 2019; Kesen, 2021; Hoseinnezhad et al, 2020). Markus plane-parallel ionization chamber with model TN23343-3795 was used in this study for depth dose measurement. It is manufactured in the original Markus design and the thin entrance window allows dose measurements in solid state phantoms up to the surface. This ionization chamber has a sensitivity volume of 0.055 cm^3 and the total window area density is 1.06 mg/cm^2 including the protection cap (Keivan et al., 2018). This ionization chamber was calibrated traceably to SSDL in ANM. Ionization chamber was used together with an electrometer for dose measurement. Electrometer is a device that collects charges ionized by radiation in the ionization chamber. The collected charges will be multiplied

with the calibration coefficient from the certificate of calibration in Appendix D to get measured doses accurately.



Figure 3.6: Markus plane-parallel ionization chamber

3.3 Water-equivalent RW3 Slab Phantom

The solid water phantom used in this study is the RW 3 phantom, which is water-equivalent and having 1.04 g/cm^3 density, suitable for high energy photon and electron dosimetry (Ispir et al., 2021). Depth dose measurement using this phantom is available as the thicknesses of the slabs composing this phantom are 1mm, 2mm, 5mm, 10mm, 40mm and 50mm. Hence, it is fine to measure depth doses with varying depths by changing the composition of the slabs. The adapter plate for the ionization chamber is 2 mm thick and the dimension of the complete phantom is 30 cm x 30 cm x 30 cm.



Figure 3.7: RW 3 solid water phantom

3.4 Metal Plates and Superflab Bolus

The metal objects used in this research were aluminium and lead with different thickness by referring to the material of metallic implants. Clinically, aluminium is used as a major alloying element with titanium for orthopedic implants. There are no lead implants, but some metallic implants are made of materials with high density and atomic numbers similar to or higher than lead such as gold, which is used as dental prostheses. Figure 3.8 and Table 3.1 show the information of metal plates used in this study.

Table 3.1: Physical characteristics of metal plates

Material	Atomic number	Density (g/cm ³)	Dimension (cm ³)
Aluminium	13	2.7	7 x 7 x 0.5
			7 x 7 x 1.0
Lead	82	11.35	5.5 x 5.5 x 0.5

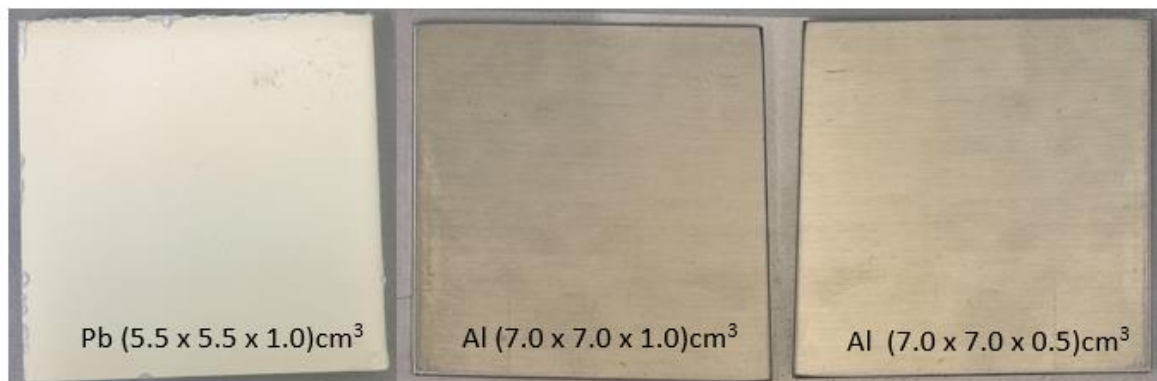


Figure 3.8: Lead and aluminium plates with different thicknesses

A 0.5 cm thick and 30 cm x 30 cm superflab bolus was involved. It is made of synthetic oil gel that can conform completely to a variety of uneven surface geometries while eliminating air gaps. The bolus is also elastic, optimizing dose build-up and help maintains uniform thickness. Hence, the bolus was put above the metal materials to remove the air gap between the slab phantom and metal surface while properly place the metal plates inside the phantoms.

3.5 Dose Measurement Without Metal Plates

Homogeneity is a medium with identical density. A homogenous medium was established by 20cm solid water phantom without the presence of metal plates. The electrometer was prepared outside the treatment room and set with 300V polarity, it was then connected to the IC in the treatment room. IC was put and fixed into the adapter plate, which was put at the top of the phantom and aligned with the lasers as shown in Figure 3.9. Irradiations started with ionization chamber measurement first along the central axis of the phantom. The irradiation parameters were 6 MV photon beam, 0° collimator angle, 0° gantry angle, 0° couch angle, 100 monitor unit (MU), 100 cm Source-to-surface distance (SSD) and 5 cm x 5 cm field size. The depths selected for IC measurements were 0 cm, 1.0 cm, 1.5 cm, 2.0 cm, 2.5 cm, 3.0 cm, 4.0 cm, 5.0 cm, 5.5 cm, 6.0 cm, 7.0 cm, 8.0 cm, 9.0 cm, 10.0 cm, 12.0 cm, 14.0 cm and 15.0 cm. The collected charges from the electrometer were recorded. After IC measurements, OSLDs measurements was continued with the same irradiation parameters. The measurement depths of OSLDs were the same as IC measurements but excluding 10.0 cm and 14.0 cm depths due to the limitation of the number of OSLDs. Hence, 30 nanodot dosimeters were used in which two OSLDs were put at the cross-hair of the light beam at each measurement depths. During the readout process, each OSLD was read three times. The OSL response for each measurement depth was taken as the average of six readings.

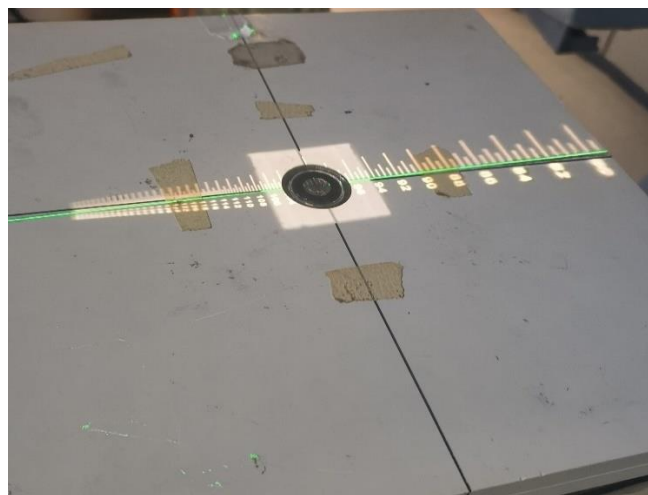


Figure 3.9: Alignment of the IC adapter plate to the lasers

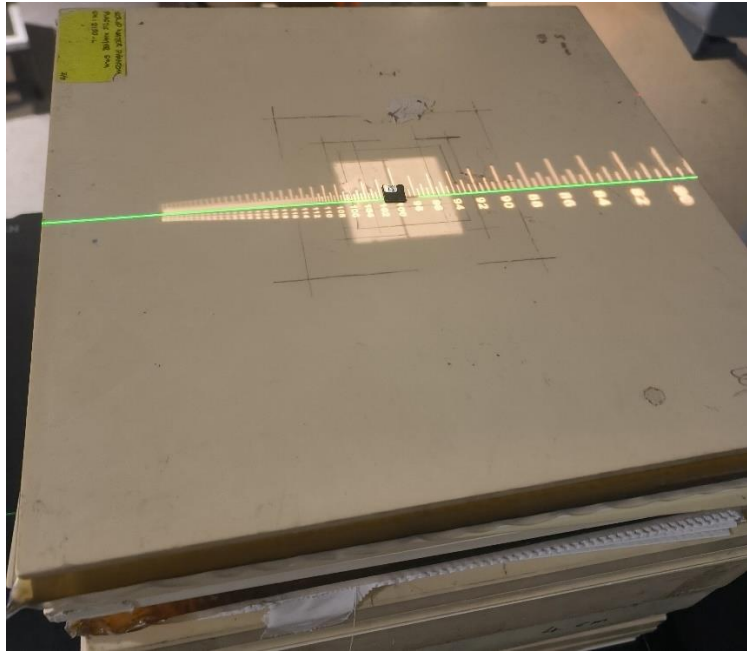


Figure 3.10: Placement of nanodot dosimeters at the cross-hair of the light beam

Finally, OSL doses were compared to IC doses. Their PDD were plotted as well based on the Equation (1) in which PDD is defined as the quotient of dose at any depth to the dose at a reference depth along the central axis of the beam. The reference depth selected was usually the depth of maximum dose (d_{max}).

$$PDD = \frac{D_d}{D_{max}} \times 100\%$$

(1)

3.6 Dose Measurement in the Presence of Metal Plates

Heterogeneity is a medium with different density and it was established by putting metal plates in the phantom, creating an interface of high-low density. Aluminium and lead were selected as the metal materials to evaluate the dose perturbation of high photon energy beam. In a 20 cm solid water phantom, certain slab phantom was replaced by metal plates at a depth of 5.0 cm, a superflab bolus with 0.5cm thickness was put above the metal materials. The irradiation started with IC and OSLDs measurement in the presence of 0.5 cm aluminium plate first followed by 1.0 cm aluminium and 1.0 cm lead plate, the thickness of phantom was 20 cm for all measurement setup. The irradiation parameters were the same as section 3.5. Figure 3.11 to

3.13 illustrated the measurement depths for IC and OSLDs dosimetry in the presence of metal plates.

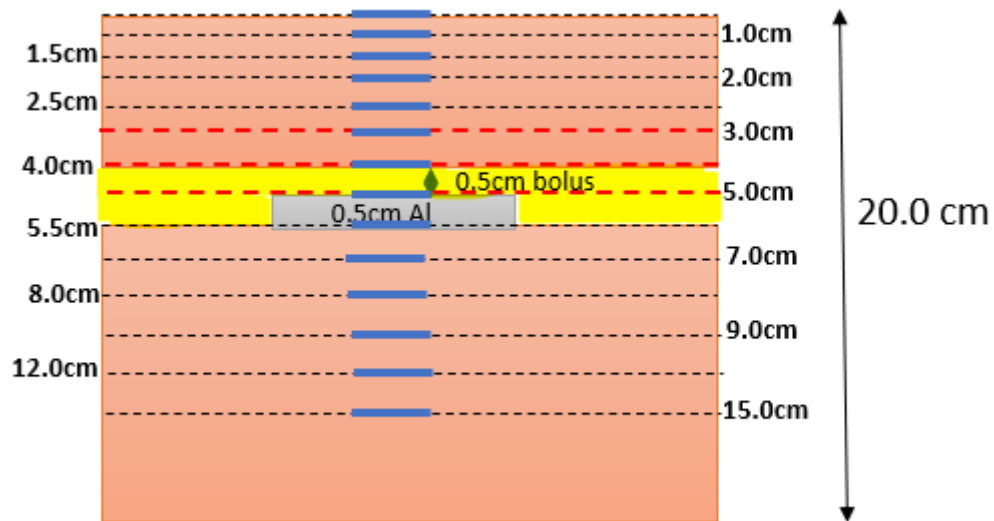


Figure 3.11: Dose measurements in the presence of 0.5 cm thick aluminium plate

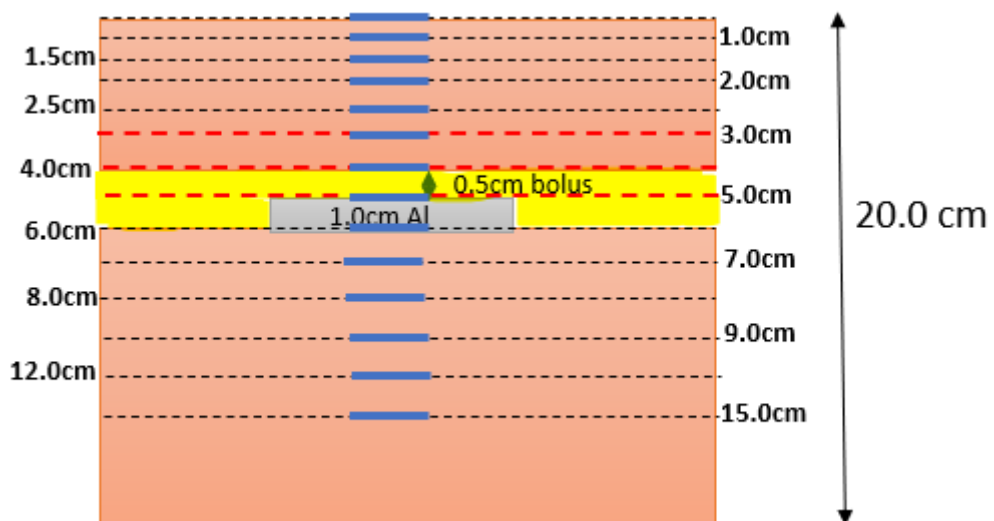


Figure 3.12: Dose measurements in the presence of 1.0 cm thick aluminium plate

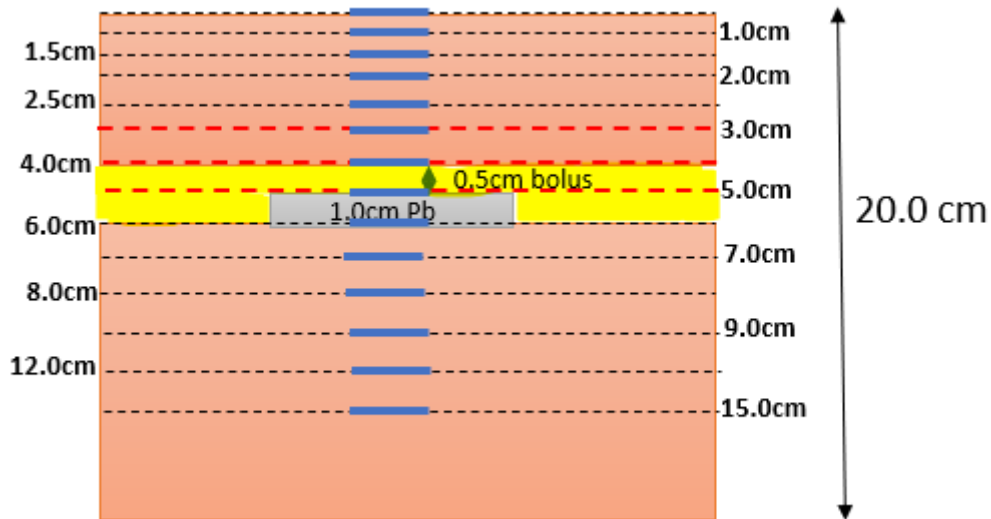


Figure 3.13: Dose measurements in the presence of 1.0 cm thick lead plate

Figure 3.11, 3.12 and 3.13 showed depth dose measurements in the presence of metal plates. The normal dash lines were both IC and OSLDs measurements. The bolded dash lines with red colour were OSLDs measurements only. This was because the 2 cm thick adapter plate plus a 0.5 cm bolus made 2.5 cm depth be the nearest distance of measurements of IC to the upper interface as shown in Figure 3.15. Finally, OSL measured doses and PDD were compared to IC measurement. PDD calculation was referred to Equation 1. Other than comparisons of measured doses and PDD between OSLDs and IC dosimetry, dose perturbation due to the metal objects were studied as well. In this case, PDD from OSLDs measurements with and without the metal plates were compared and analyzed. Besides, several depth doses of OSL measurement before and after the high-low density interface were selected to compare the doses with and without the metal plates. The comparisons were done through a dose perturbation factor (DPF). DPF is defined as the ratio of dose to a point in an inhomogeneous medium to the same point within a homogeneous medium (Ade & Du Plessis, 2017). In this case, metal objects were involved to study the impact of metal-related inhomogeneity on dose distribution. Hence, DPF were separated into two components, which were backscatter dose perturbation factor (BSDF) for depth dose comparisons near to the entrance of the high-low density interface (2.5 cm, 3.0 cm, 4.0 cm and 5.0 cm) and forward dose perturbation factor

(FDPF) for depth dose comparisons after the high-low density interface (5.5 cm to 15.0 cm). Their calculations were shown by Equation (2) and (3) where D_i is the dose with the presence of metal objects while D_h is the dose without the presence of metal objects. Furthermore, percentage differences were determined for comparison of the measured doses and PDD between IC and OSL dosimetry in all measurements with and without metal plates. The calculations of percentage differences for doses and PDD are shown by Equation (4) and (5) respectively.

$$BSDF = \frac{D_i}{D_h} \tag{2}$$

$$FDPF = \frac{D_i}{D_h} \tag{3}$$

$$\left(\frac{D_{OSL} - D_{IC}}{D_{IC}} \right) \times 100\% \tag{4}$$

$$\left(\frac{PDD_{OSL} - PDD_{IC}}{PDD_{IC}} \right) \times 100\% \tag{5}$$

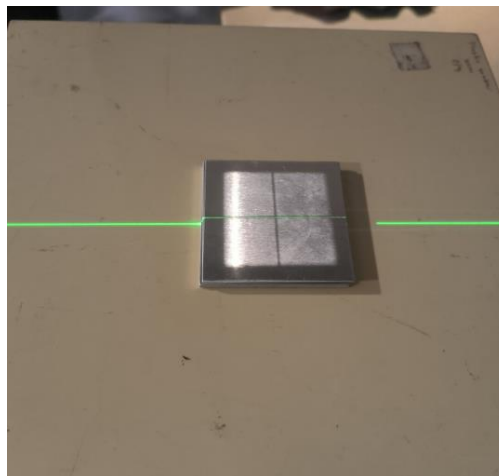


Figure 3.14: Centralization of 0.5 cm aluminium plate to the cross-hair of the light field



Figure 3.15: IC measurements in the presence of metal plates



Figure 3.16: OSL measurements in the presence of metal plates

3.7 Study Flowchart

Figure 3.17 showed the flowchart of this study, starting from the identification of the title until the completion of thesis writing.

